# Engineered Antibodies of IgG1/IgG3 Mixed Isotype with Enhanced Cytotoxic Activities

Akito Natsume,[1] Mika In,[3] Hiroyuki Takamura,[4] Tomoaki Nakagawa,[1] Yukiko Shimizu,[1] Kazuko Kitajima,[1] Masako Wakitani,[1] So Ohta,[1] Mitsuo Satoh,[1] Kenya Shitara,[2] and Rinpei Niwa[1]

[1]Antibody Research Laboratories, Pharmaceutical Research Center and [2]Antibody Business Office, Pharmaceuticals Business Unit, Kyowa Hakko Kogyo Co. Ltd., Tokyo, Japan; [3]Toxicological Research Laboratories, Ube Branch Pharmaceutical Research Center, Kyowa Hakko Kogyo Co. Ltd., Yamaguchi, Japan; and [4]Pharmacokinetic Research Laboratories, Pharmaceutical Research Center, Kyowa Hakko Kogyo Co. Ltd., Shizuoka, Japan

## Abstract

**Enhancement of multiple effector functions of an antibody may be a promising approach for antibody therapy. We have previously reported that fucose removal from Fc-linked oligosaccharides greatly enhances antibody-dependent cellular cytotoxicity (ADCC) of therapeutic antibodies. Here, we report a unique approach to enhance complement-dependent cytotoxicity (CDC), another important effector function of antitumor antibodies, by using engineered constant region of human IgG1/IgG3 chimeric isotypes. We systematically shuffled constant domains of IgG1 and IgG3 to generate a comprehensive set of mixed chimeric isotypes of anti-CD20 antibodies. Among these, the variant 1133, consisting of the CH1 and the hinge each from IgG1 and the Fc from IgG3, was unexpectedly found to exhibit markedly enhanced CDC that exceeded wild-type levels. However, it lacked protein A–binding capacity, an important feature for the industrial production. To eliminate this deficiency, a portion in COOH-terminal CH3 domain of 1133 was substituted with IgG1, resulting in full recovery of protein A binding without compromising the enhanced CDC and ADCC activities. The CDC-enhancing effect using a chimeric isotype was also shown in CD52 antigen/antibody system. The ADCC activity of the variants was also maximized by the absence of fucose from its carbohydrate structure, a phenomenon that has previously been observed for wild-type antibodies. Enhanced cytotoxicity of a variant was confirmed in a cynomolgus monkey model. These findings suggest that the variant antibodies with IgG1/IgG3 chimeric constant regions and nonfucosylated oligosaccharides that possess dual-enhanced cytotoxic functions may be an improvement for the next generation of therapeutic antitumor antibodies.** [Cancer Res 2008;68(10):3863–72]

## Introduction

Therapeutic antibodies, such as chimeric, humanized, and fully human antibodies, typically use for its backbone structure the human IgG1 constant region. This isotype was chosen primarily because of its capacity to induce strong effector functions in humans, such as antibody-dependent cellular cytotoxicity (ADCC) and complement-dependent cytotoxicity (CDC).

Recent studies have suggested the importance of these effector functions in antibody therapy (1–4). The most validated and well-characterized effector function in the clinic may be the mechanisms dependent on Fcγ receptor (FcγR) IIIa, a receptor present on natural killer (NK) cells, monocytes/macrophages, and dendritic cells. Several studies have shown a relationship between therapeutic efficacy and functional polymorphism of FcγRIIIa (2, 5–7). Because FcγRIIIa on NK cells is the major receptor that triggers ADCC, extensive efforts have been made to improve FcγRIIIa-binding affinity of IgG1 constant region to enhance ADCC, including random or rational amino acid mutations (8, 9) and modification of oligosaccharides linked to $Asn^{297}$ in the Fc (10–12). Of these, removal of fucose from Fc-linked oligosaccharides might be one of the most powerful approaches. In mammals, fucose residues are attached to innermost GlcNAc residue of almost all complex-type Asn-linked oligosaccharides via an α1,6 linkage (13). We have previously shown that fucose is the most critical component of antibody oligosaccharide for ADCC, and removal of fucose from human IgG1 antibodies significantly augments FcγRIIIa binding (14), enhances ADCC by as much as ~100-fold *in vitro* (12), and improves antitumor activity *in vivo* (15). The effect is not limited to IgG1 but also applicable to other IgG isotypes (16) or antibody-like binding molecules having Fc (17, 18). For the production of nonfucosylated antibodies, we have generated an α1,6-fucosyltransferase gene (*FUT8*) knockout Chinese hamster ovary (CHO) cell line (CHO/$FUT8^{-/-}$), which can stably produce nonfucosylated antibodies (known as Potelligent technology; ref. 19). Conventional therapeutic antibodies produced with wild-type CHO cells posses almost fully fucosylated oligosaccharides and exhibit only modest ADCC (11, 12).

CDC is a cytolytic cascade mediated by a series of complement proteins C1 to C9 abundantly present in serum, and triggered by binding of C1q to the Fc region of antibody molecules bound on the cell surface. Several studies have shown that CDC can be enhanced by facilitation of this initial step by using designed antibody constant regions, which possess improved C1q binding as a result of engineered, amino acid mutations inserted either into the Fc (20) or into the hinge region (21). Alternatively, partial or whole deletion of hinge sequences in human IgG3 also resulted in an increase in CDC activity (22, 23).

Apart from amino acid and structural idiosyncrasies, the four isotypes of human IgG differ from each other in the potencies of effector functions and other activities (16, 24, 25). In general, the rank order of potency is IgG1 ≧ IgG3 ≫ IgG4 ≧ IgG2 for ADCC (16, 26) and IgG3 ≧ IgG1 ≫ IgG2 ≒ IgG4 for CDC (16, 24, 25). Using these functional differences, structural shuffling between isotypes has been actively studied to generate chimeric isotypes

**Requests for reprints:** Rinpei Niwa, Antibody Research Laboratories, Pharmaceutical Research Center, Kyowa Hakko Kogyo Co. Ltd., 3-6-6 Asahi-machi, Machida-shi, Tokyo 194-8533, Japan. Phone: 81-42-725-2555; Fax: 81-42-725-2689; E-mail: rinpei.niwa@kyowa.co.jp.



doi:10.1158/0008-5472.CAN-07-6297

with various altered functions of antibody (e.g., IgG1/IgG4, IgG2/IgG3, or IgG3/IgG4 shuffling; refs. 27–31). It seems reasonable to expect that these modifications rarely generate enhanced functions that exceed wild-type levels. One exception is an observation in which introduction of IgG4 hinge into IgG3 significantly enhanced CDC activity that was more potent than either IgG3 or IgG4 (31), although another group reported conflicting results with the null effect on CDC by the same structure (30). Because many of these studies were intended to determine the essential sites for the activities of interest, the methods tended to be combinations of active/inactive isotypes. Thus, systematic shuffling to create mixed isotypes, which retain the effector functions characteristics of each type such as IgG1/IgG3 or IgG2/IgG4, is poorly studied.

In this report, we describe a unique approach to create a panel of variant heavy chain constant regions with highly diverse profiles of effector functions by shuffling human IgG1 and IgG3 isotypes to generate a comprehensive set of variant anti-CD20 antibodies of mixed chimeric isotypes. Among these variants, we found some constructs that showed particularly potent CDC activity. Additionally, maximal ADCC was retained by producing antibodies in the CHO/*FUT8*$^{-/-}$ cells that stably produce nonfucosylated antibodies. Thus, antibodies with variant constant regions of potentially improved therapeutic value in which ADCC and CDC are simultaneously enhanced have been successfully generated.

## Materials and Methods

**Cell lines.** CHO/DG44, a wild-type CHO cell line (32), was kindly provided by Dr. Lawrence Chasin (Columbia University, New York, NY). CHO/*FUT8*$^{-/-}$, α1,6-fucosyltransferase gene (*FUT8*) knockout CHO cells for production of IgG without fucosylation, has been described previously (19). Human CD20$^+$ B lymphoma Raji, ST486, and Daudi were purchased from the American Type Culture Collection. CD20-transfected CD20/EL4 cells were described previously (33). Human CD52$^+$ chronic B-cell leukemia EHEB and MEC-1 were purchased from the German Collection of Microorganisms and Cell Cultures.

**Blood donors.** Blood donors were randomly selected from healthy volunteers registered in Kyowa Hakko Kogyo Co. Ltd. All donors gave written informed consent before analyses, in accordance with the process approved by the institutional Ethical Committee.

**Establishment of cells producing human IgG1/IgG3 chimeric isotype antibodies.** Stable expression vectors for anti-CD20 human IgG1/IgG3 chimeric isotype antibodies were generated by substituting a part of heavy chain gene in the expression vector for anti-CD20 human IgG1 antibody (12) with the corresponding part of IgG3 heavy chain gene (Genbank accession no. AAH53984). The genes of the modified heavy chain constant regions and κ light chain constant region were each joined to genes encoding identical amino acid sequences of variable regions of a therapeutic anti-CD20 antibody rituximab (light chain variable region: Genbank accession no. AR015962; heavy chain variable region: Genbank accession no. AR000013). Scheme of the variant heavy chain constant regions constructed in this study is shown in Fig. 1. The segmentation of each domain was according to the EU numbering by Kabat et al. (34). In the set of variants in which the whole CH2 domain and a part of $NH_2$-terminal region of the CH3 domain were converted to IgG3 (variants 113A to 113G; Fig. 1), the segmentation in the CH3 was set according to amino acid residues that are different in IgG1 and IgG3 (i.e., the IgG3-converted region in each variant was located from the $NH_2$ terminus of the CH2 domain to positions 356, 358, 384, 392, 397, 422, or 435 for variants 113A, 113B, 113C, 113D, 113E, 113F, or 113G, respectively). For the generation of expression vectors of anti-CD52 antibodies, the variable region genes of anti-CD20 antibody expression vector with wild-type or modified heavy chains were replaced with those of an anti-CD52 antibody alemtuzumab (light chain variable region: Genbank accession no. S79311; heavy chain variable region: Genbank accession no. S79307). The expression vectors were then introduced into CHO/DG44 or CHO/*FUT8*$^{-/-}$ cells (19) via electroporation, and high-producing clones were selected as described previously (16, 19).

**Production and purification of fucose variants of human IgG1/IgG3 chimeric isotype antibodies.** Transfectant clones were cultured, and the antibodies were then purified from the supernatants using protein G-Sepharose (Millipore). The purified anti-CD20 antibodies were designated as listed in Fig. 1. Anti-CD52 human IgG1 antibody and 113F version of anti-CD52 antibody were designated as CD52-IgG1wt and CD52-113F, respectively. The monosaccharide composition analysis of Asn-linked oligosaccharides was performed as described previously (16, 19). For a fucosylated anti-CD20 IgG1 antibody, commercially available rituximab (Genentech) was used in this study (Fig. 1, designated as IgG1wt-fucosylated).

**Measurement of CD20-binding activity.** CD20-binding analysis was performed by a competitive flow cytometry method. Briefly, Raji cells ($5 \times 10^5$) were incubated with various concentrations of anti-CD20 antibody or anti-CD52 human IgG1 control antibody (CD52-IgG1) in the presence of 0.5 μg/mL of biotinylated anti-CD20 antibody (16) for 1 h on ice. After washing, biotinylated anti-CD20 antibody bound on the cell surface was detected by EPICS XL-MCL flow cytometer (Beckman Coulter) using phycoerythrin (PE)-labeled streptavidin (Beckman Coulter).

**ADCC assay.** Peripheral blood mononuclear cells (PBMC) were prepared from blood of healthy volunteers by Lymphoprep (Axis Shield). Target cells ($1 \times 10^4$) were incubated with various concentrations of anti-CD20 antibody and human PBMC as effector cells at an E:T ratio of 20:1 for 4 h at 37°C. After incubation, the target cells lysed by ADCC were detected by the lactate dehydrogenase release assay and the percent cytotoxicity was calculated as described previously (19).

**CDC assay.** CDC assay was performed as described previously (16). Briefly, target cells ($5 \times 10^4$) were incubated with various concentrations of anti-CD20 antibody and human serum (Sigma) as the source of complement at a dilution of 1:6 in supplemented RPMI 1640 for 2 h at 37°C in 96-well flat-bottomed plates. After incubation, the cell proliferation reagent WST-1 (Roche Diagnostic GmbH) was added (15 μL/well) and the plates were further incubated for 4 h to detect the live cells. The absorbance ($A_{450}$-$A_{650}$) of the formazan dye produced by metabolically active cells of each well was detected on an Emax plate reader (Molecular Devices). Cytotoxicity was calculated according to the following formula: % cytotoxicity = $100 \times (E - S) / (M - S)$, where $E$ is the absorbance of experimental well, $S$ is that in the absence of monoclonal antibody (cells were incubated with medium and complement alone), and $M$ is that of medium and complement in the absence of target cells and antibody.

**Protein A–binding assay.** ELISA plates were coated with 5 μg/mL of goat anti-human κ light chain antibody (Sigma) in PBS (50 μL/well) for 1 h at room temperature and washed with PBS for three times. Then, the plates were blocked with 100 μL/well of PBS containing 1% bovine serum albumin (1%BSA-PBS) for 1 h. After blocking, various concentrations of anti-CD20 antibody in 1%BSA-PBS (50 μL/well) were incubated on the plates for 1 h at room temperature and washed with PBS containing 0.05% Tween 20 (wash buffer) for five times. Horseradish peroxidase (HRP)-labeled protein A (Amersham Bioscience) at a dilution of 1:5,000 in 1%BSA-PBS (50 μL/well) were added and incubated for 30 min at 37°C. After washing, bound protein A was detected with ABTS as the substrate, and absorbance at 415 nm was measured on an Emax plate reader.

**Complement-binding assay.** CD20$^+$ Daudi cells ($10^6$) were incubated with various concentrations of anti-CD20 antibody in supplemented RPMI 1640 (150 μL/well) for 10 min at room temperature, and 50 μL/well of human serum (Sigma) diluted to 4% (v/v) were added and incubated for 15 min at 37°C. Cells were then washed with PBS for two times and incubated with FITC-labeled anti-C1q or anti-C4b antibody (DakoCytomation) at a dilution of 1:200 for 1 h on ice. After washing with PBS for two times, stained cells were detected by EPICS XL-MCL flow cytometer.

**FcγR-binding assay.** Binding activity of anti-CD20 antibodies to recombinant FcγRI, FcγRIIa ($^{131}$His allotype), FcγRIIb, and FcγRIIIa ($^{158}$Val allotype) was determined by an ELISA method as described previously (14). Briefly, ELISA plates were coated with 5 μg/mL of anti-Tetra His antibodies (Qiagen) in PBS. After blocking with 1%BSA-PBS,

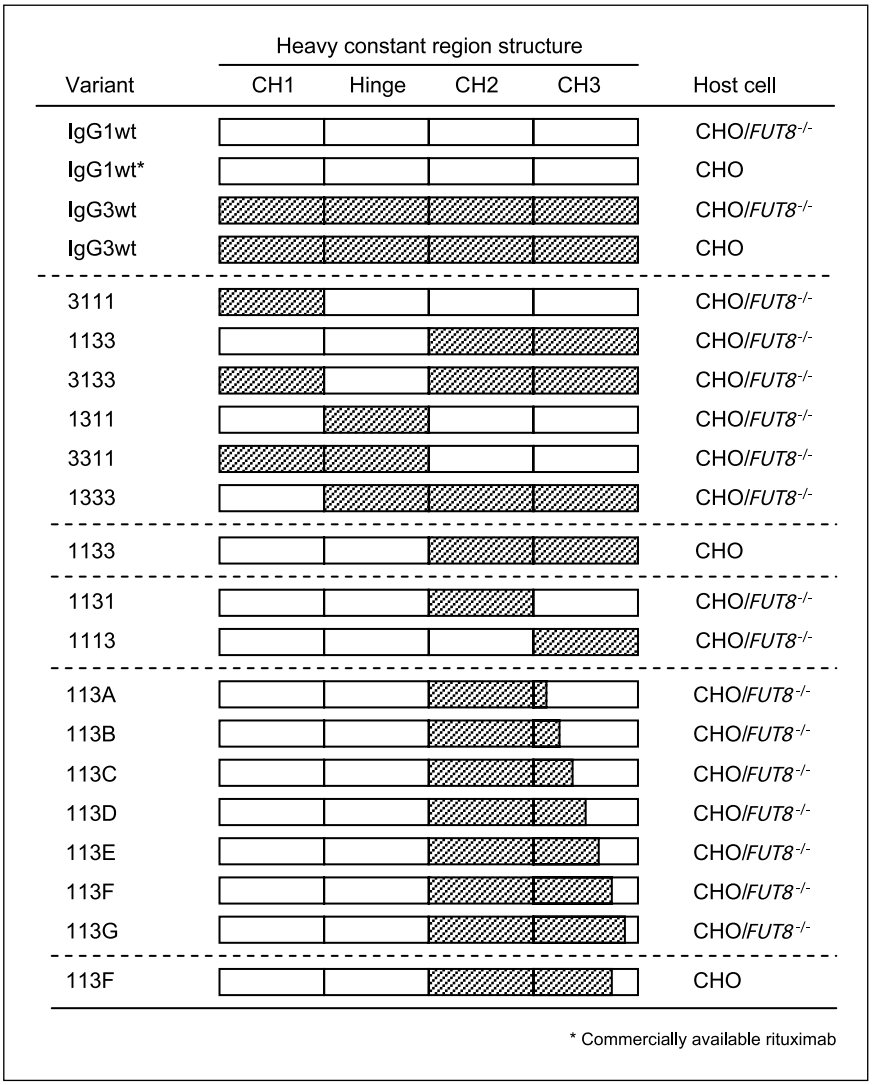


**Figure 1.** Scheme of the chimeric isotype antibodies constructed in this study. Open squares and hatched squares represent domains derived from human IgG1 and IgG3, respectively. All antibodies share variable regions of rituximab and light chain constant region of $C_\kappa$ isotype (data not shown).

recombinant $His_6$-tagged receptors were incubated on the plates at room temperature for 2 h. After washing, various concentrations of antibodies were added and incubated at room temperature for 2 h. After washing, bound antibodies were detected using HRP-labeled goat anti-human IgG (H+L) antibodies (American Qualex). Absorbance at 415 nm was measured on an Emax plate reader.

**Monkey study.** Animal experiments were performed in conformity with institutional guidelines in compliance with national laws and policies. Eight cynomolgus monkeys were given single i.v. injection of IgG1wt or variant 113F anti-CD20 ($n$ = 4 per group) at a dose of 0.1 mg/kg. Blood samples were collected on two separate days (days −7 and −1) before administration for the determination of predosing values and at 6 h and days 1, 2, 5, 14, 28, and 56 after injection. Each sample was stained with excess FITC-conjugated anti-CD20 antibody (clone Leu16) and PE-conjugated anti-CD3 antibody, and then viable B cells ($CD20^+CD3^-$) and T cells ($CD20^-CD3^+$) were quantified with flow cytometry in the presence of a fixed number of FlowCount beads (Beckman Coulter) as an internal standard for quantification.

## Results

**Design and expression of a panel of variant antibodies of IgG1/IgG3 chimeric isotype.** We designed a set of the heavy chain constant regions in which CH1, hinge, Fc domains were shuffled between IgG1 and IgG3 (Fig. 1; variants 3111, 1133, 3133, 1311, 3311, and 1333). The numerals in the names correspond to the IgG subclass of each domain in the order of CH1/hinge/CH2/CH3. These designed heavy chain constant regions were expressed with identical VH domain and light chain both derived from rituximab (35), a therapeutic anti-CD20 antibody, using CHO/*FUT8*$^{-/-}$ cells (19) as host cells. We have previously shown that nonfucosylated human IgG antibodies produced in this expression system significantly enhance ADCC irrespective of their subclass while not affecting other functions, such as antigen binding and CDC (16). Expression vectors encoding some of the antibodies were also introduced into wild-type CHO cells (CHO/DG44 cells) as host cells to generate antibodies with conventional fucosylated oligosaccharides (Fig. 1).

Purified antibodies produced with CHO/*FUT8*$^{-/-}$ cells were then subjected to monosaccharide composition analysis. Consistent with prior studies (16–19), we confirmed that fucose was not detected in complex-type Asn-linked oligosaccharides of antibodies, whereas majority (>90%) of Asn-linked oligosaccharides of all antibodies produced with wild-type CHO cells were fucosylated. The contents of other monosaccharide components that constitute Asn-linked oligosaccharides of antibody (mannose, galactose, and

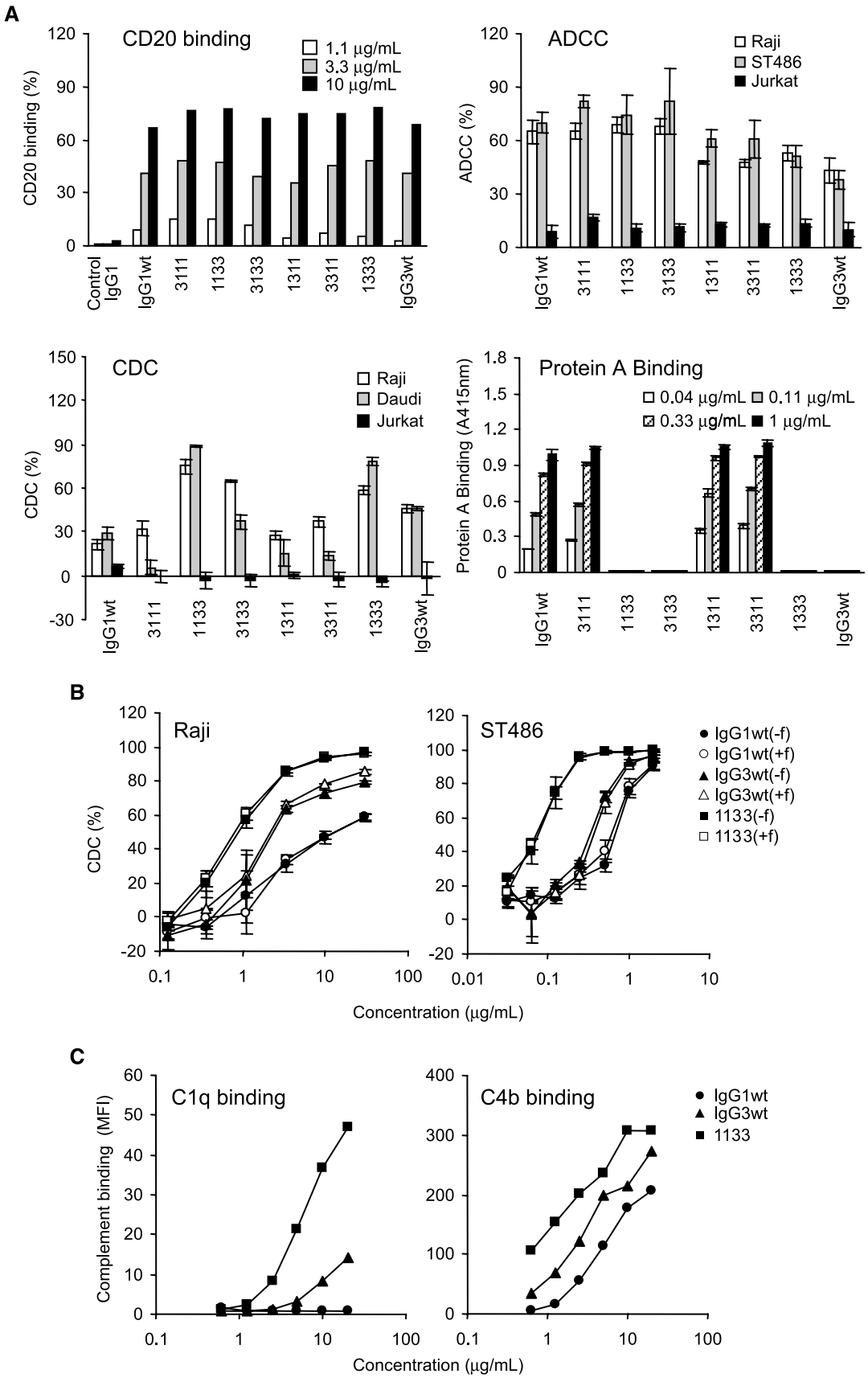

*N*-acetylglucosamine) did not significantly vary among the antibody samples (data not shown).

All heavy chain and light chain proteins were expressed at expected molecular sizes confirmed by SDS-PAGE analysis (data not shown).

**Various activities of human IgG1/IgG3 chimeric isotype antibodies.** Various biological functions of the domain-shuffled anti-CD20 variants were then investigated. For the cell-based assays, four $CD20^+$ lymphoma cell lines were used in this study; the numbers of CD20-binding sites per cell are $4.0 \times 10^5$, $5.9 \times 10^5$, $3.2 \times 10^5$, and $1.2 \times 10^4$ for Raji, Daudi, ST486, and murine transfectant CD20/EL4-A, respectively (as determined in a previous study; ref. 33). Although all the variants and wild-type antibodies were very similar in CD20-binding activity (Fig. 2*A*), substantial differences were seen among variants in other functions. As for ADCC, all the wild-type and the variant antibodies had nonfucosylated glycoform and therefore were expected to have enhanced cytotoxic activity; however, there still were differences in activity among variants (Fig. 2*A*). They were roughly divided into two groups according to their structures: (*a*) constructs with IgG1 hinge (variants 3111, 1131, and 3133) with potent activity as that of IgG1wt and (*b*) constructs with IgG3 hinge (variants 1311, 3311, and 1333) with relatively lower activity as that of IgG3wt, as shown in two $CD20^+$ lymphoma cell lines tested (Raji and ST486). This suggests that the introduction of IgG3 hinge seems to decrease ADCC to a similar level to that of IgG3wt. No cytotoxic activity was shown in $CD20^-$ Jurkat cells for both assays.

Of particular interest were three constructs that possessed the Fc of IgG3 (variants 1133, 3133, and 1333) unexpectedly showed remarkable CDC activity exceeding the parental wild-type antibodies (IgG1wt and IgG3wt; Fig. 2*A*). Of these, the variant 1133, composed of CH1 and hinge both derived from IgG1 and the Fc derived from IgG3, showed the highest CDC activity against both Raji and Daudi cells. Variant 1333 showed the second best activity, and the third variant 3133 showed enhanced CDC only against Raji cells. Importantly, variant 1133, in addition to having the best CDC activity, was also capable of mediating strong ADCC comparable with IgG1wt. However, these CDC-enhancing variants with IgG3 Fc did not bind protein A as well as IgG3wt (Fig. 2*A*). This deficiency would greatly compromise the purification efficiency in the industrial production processes.

**Enhanced CDC activity of variant 1133.** Among the variant antibodies with shuffled constant regions, the variant 1133 had the most desirable profile with respect to its potential for therapeutic use because it displayed enhanced CDC while retaining maximized ADCC capacity similar to that of nonfucosylated IgG1. Additional analysis of CDC activity at varying concentrations revealed that this variant exhibits markedly higher activity than both parental IgG1 and IgG3 (Fig. 2*B*). As expected, the absence or presence of fucose in the oligosaccharides linked to the Fc did not affect CDC of any of the antibodies.

In parallel with enhanced CDC activity, variant 1133 showed increased binding to C1q, the initial complement component in the classic pathway, and consequently fixed more C4, a downstream component (Fig. 2*C*), suggesting that the variant constant regions have enhanced capacity to bind to C1q. This assay system was not sensitive enough to detect C1q weakly bound to IgG1wt.

**Further modification of variant 1133 that confers protein A–binding capacity.** Additional studies were carried out to determine if enhanced CDC activity and protein A–binding capacity could be combined in the same antibody construct. In this context, two IgG3-derived domains in the variant 1133 (CH2 and CH3) were individually converted to IgG1 and tested for the desired activity (variants 1131 and 1113; see Fig. 1).

As shown in Fig. 3*A*, variant 1131 exhibited slightly decreased CDC compared with 1133, but still much more potent than IgG1wt. Another variant, 1113, also showed higher CDC activity than IgG1wt; however, the degree of enhancement was lower than that seen for 1131. This indicates that, although both domains in the Fc were involved in the enhancement, the conversion of the CH2 domain into IgG3 was more effective to enhance CDC than that in the CH3 domain.

In the next set of variants, the COOH-terminal region of the CH3 domain in 1133 was converted to IgG1 in a stepwise manner, aiming to obtain maximal CDC without losing protein A binding (Fig. 1, variants 113A to 113G). To compare CDC activities of these variants, assays were performed using CD20-transfected EL4 cells, which expressed significantly lower levels of CD20 (described above). In this experiment, the differences in CDC activity between variants 1133 and 1131 were more dramatically revealed using the transfected EL4 cells than when the natural lymphoma cell line (Raji) was used. Among these, CDC activities of the variants, in which the length of IgG3-converted region was relatively shorter (113A to 113D), were seen at levels as low as shown for variant 1131. For other variants (113E, 113F, and 113G), CDC activity was shown to be proportional to the length of the IgG3 regions, with the maximal level of cytotoxicity for 113G being almost equivalent to 1133 (Fig. 3*B*). All the variants except 113G showed protein A–binding activity (Fig. 3*B*).

Finally, the variant 113F had the best CDC activity among all the variants that bind to protein A. The enhanced CDC activity of variant 113F and its fucosylated version was also confirmed in a natural human cell line (Raji) irrespective of their glycoform, in parallel with the improved C1q/C4b binding on the cell surface (Fig. 3*C*). Quantitative analyses with repeated experiments revealed that variant 113F, as well as its parental variant 1133, shows ~10-fold (against ST486 cells) or ~50-fold lower (against Raji cells) $EC_{50}$ values for CDC activity than IgG1wt. In addition, saturating cytotoxic activity achieved at higher concentrations

**Figure 2.** Effect of IgG1/IgG3 isotype shuffling on functions of an anti-CD20 antibody. *A,* various activities of human IgG1/IgG3 chimeric isotype antibodies. All antibodies shown were produced using CHO/*FUT8*$^{-/-}$ cells as host cells and consequently have nonfucosylated glycoform. *Top left,* binding activity of anti-CD20 human IgG1/IgG3 chimeric isotype antibodies or anti-CD52 IgG1wt (as a negative control) to Raji cells at various concentrations. *Top right,* ADCC activity of anti-CD20 antibodies against Raji (*open columns*), ST486 (*hatched columns*), and Jurkat ($CD20^-$ target; *filled columns*) cells in the presence of 0.1 μg/mL (for Raji and Jurkat) or 0.01 μg/mL (for ST486). *Bottom left,* CDC activity against Raji (*open columns*), Daudi (*hatched columns*), and Jurkat ($CD20^-$ target; *filled columns*) cells in the presence of 1.25 μg/mL (for Raji), 0.16 μg/mL (for Daudi), and 3.3 μg/mL (for Jurkat) of anti-CD20 antibodies. For ADCC and CDC, similar results were also obtained at varying antibody concentrations (data not shown). *Bottom right,* binding activity of various concentrations of anti-CD20 antibodies to protein A. *Columns,* mean of triplicates; *bars,* SD. *B,* quantitative analyses on the complement-mediated functions of variant 1133 in comparison with wild-type antibodies. CDC activity of IgG1wt, IgG3wt, and variant 1133 of both fucosylated [*open symbols*: "(+f)" samples] and nonfucosylated glycoforms [*closed symbols*: "(−f)" samples] against Raji (*left*) and ST486 (*right*) cells. *Points,* mean of triplicates; *bars,* SD. *C,* binding of complement proteins C1q (*left*) and C4b (*right*) on Daudi cells coated by anti-CD20 antibodies. All antibodies shown have nonfucosylated glycoform. Data are representative of two independent experiments. *MFI,* mean fluorescence intensity.

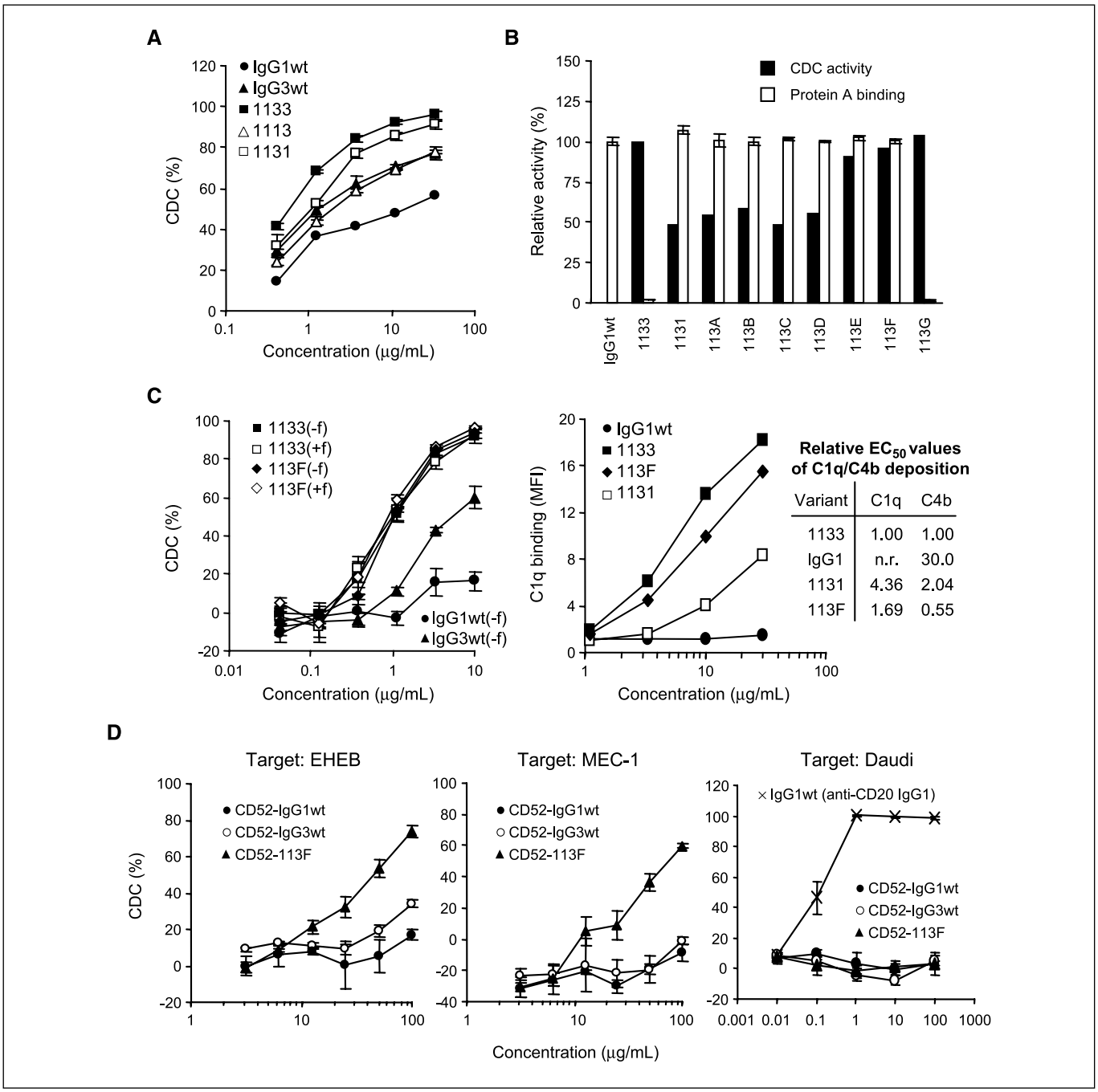


**Figure 3.** Further modification of the CH3 domain that confers protein A binding. All antibody samples shown have nonfucosylated glycoform if not otherwise specified, except in comparative studies of fucosylated and nonfucosylated antibodies [in such case, samples were denoted as (+f) and (−f) in the figures, respectively]. *A,* CDC activity of variants 1131 (□) and 1113 (Δ) in comparison with IgG1wt (●), IgG3wt (▲), and variant 1133 (■) against Raji cells. *B,* relative CDC activity (*black columns*) and protein A binding (*white columns*) of the variants in which the CH3 of variant 1133 was partially reversed to IgG1. For measuring CDC, CD20/EL4-A transfectant cells were used as target cells. Values in the presence of 3.3 μg/mL for CDC or 1.1 μg/mL for protein A were normalized to variant 1133 = 100% for CDC and IgG1wt = 100% for protein A binding. *C,* CDC activity (*left*) and complement binding (*right*) of anti-CD20 antibodies, including variant 113F using Raji cells as target cells. For the complement-binding study (*right*), representative data of actual C1q-binding plot together with relative $EC_{50}$ values of C1q/C4b deposition of each variant (*inset*) on Raji cells are shown. $EC_{50}$ value was defined as mean fluorescence intensity of each variant necessary to achieve the half-maximal binding of variant 1133 and then normalized to $EC_{50}$ of variant 1133 = 1.00. *n.r.,* not reached. Fucosylated variants showed similar C1q/C4b-binding activities to their nonfucosylated counterparts (data not shown). *D,* CDC enhancement in CD52 antibody/antigen system. CDC activity of CD52-IgG1wt (●), CD52-IgG3wt (○), and CDC-enhancing variant CD52-113F (▲) was measured using $CD52^+$ EHEB, MEC-1, and $CD52^-/CD20^+$ Daudi cells as target cells. For Daudi cells, the activity of anti-CD20 IgG1 antibody (IgG1wt) was simultaneously measured as a positive control. *Points,* mean of triplicates; *bars,* SD. All data are representative of at least two independent experiments.

was also increased for the CDC-enhancing variants against Raji cells (Table 1).

To determine if the methodology to enhance CDC, described above for anti-CD20 antibodies, can be universally applied to other antibody/antigen combinations, we generated anti-CD52 human IgG1 antibody (sample CD52-IgG1wt) and its 113F version (sample CD52-113F). For this system, we used the variable region sequences of a therapeutic humanized anti-CD52 IgG1 antibody alemtuzumab

(36), which possesses complement-activating capacity as one of the possible therapeutic mechanisms of this antibody against chronic leukemia (36, 37). We confirmed that CD52-113F showed higher CDC activity than CD52-IgG1wt against $CD52^+$ EHEB cells and MEC-1 cells (Fig. 3*D*). CD52-IgG1wt and CD52-113F showed no CDC activity in $CD52^-$ Daudi cell, but anti-CD20 IgG (IgG1wt) did exhibit CDC.

**ADCC and FcγR binding of variant antibodies.** We further performed the detailed analysis on the ADCC-inducing capacity of the CDC-enhancing variants (variants 1133, 1131, 1113, and 113F). To confirm the generality of the results, we used PBMCs purified from blood of multiple individual donors as effector cells (Fig. 4*A*, donor nos. 1–3). Fucose removal significantly increased ADCC for all antibodies tested, and as described previously (16), IgG1 showed more potent activity than IgG3 both in fucose-negative and fucose-positive settings. The variants 1133 and 113F (without fucosylation) showed very similar ADCC activity to nonfucosylated IgG1wt. Thus, the variants 1133 and 113F are endowed with potent CDC and ADCC activities enhanced by two kinds of modifications: IgG1/IgG3 chimerization in constant regions and defucosylation of the Fc-linked oligosaccharides.

Supporting the above findings, variants 1133 and 113F that were devoid of fucose in their oligosaccharides also displayed increased FcγRIIIa binding when compared with their fucose-positive counterparts (Fig. 4*B*). As for binding to FcγRI and FcγRII, these variant antibodies showed almost equal activity to that of IgG1wt, whereas fucosylation does not significantly affect the binding of all the antibodies to these receptors as seen for wild-type IgGs in previous reports (14) and in this study. Overall, FcγR-binding profile of the CDC-enhancing variants was similar to that of nonfucosylated wild-type IgG1.

**Enhanced B-cell depletion in cynomolgus monkeys.** To confirm the CDC-enhancing effect of the variant anti-CD20 antibodies *in vivo*, we first examined the CDC activities against $CD20^+$ Raji cells in the presence of murine and monkey sera (Fig. 5*A*). In concordance with previous investigation (38), murine serum was incapable of mediating measurable cytolysis even with the CDC-enhancing variant 113F. In contrast, monkey serum exhibited similar cytolytic profiles to human serum, including the increase in CDC activity by the use of the variant constant region sequences, although the difference in CDC between antibodies was slightly smaller than that observed for human serum. This suggests that monkey models might predict the therapeutic effect of the CDC-enhancing variants.

These results led us to further compare the *in vivo* effect of the variant 113F and IgG1wt (both have the same nonfucosylated glycoform) on the reduction of peripheral B cells in cynomolgus monkeys, a suitable model for the evaluation of *in vivo* efficacy of anti-human CD20 antibodies (35). As a result of single i.v. injection (0.1 mg/kg), significant enhancement in the levels of B-cell depletion was observed for 113F (Fig. 5*B*). This enhancement of B-cell depletion was manifested in a significant delay in time to recovery [e.g., % remaining B cells observed for IgG1wt at 24 h (35.0 ± 4.3%) compared with a much longer time, day 14 (31.3 ± 4.5%), observed for the animal treated with the variant antibody]. The levels of T cells ($CD20^-CD3^+$ cells) were basically unchanged during the experiment and did not show significant difference between the two groups (data not shown).

## Discussion

It has been suggested that *in vivo* effector functions of therapeutic antibodies include ADCC and CDC (1–8). Therefore, simultaneous enhancement of multiple effector functions by the use of engineered antibody sequences should be of therapeutic value. Here, we report a unique approach to enhance multiple effector functions of antibodies by recombining natural amino acid sequences and oligosaccharides that are naturally present in the antibody repertoire of humans (39). Although the actual immunogenicity of variant antibodies cannot be reliably predicted before clinical trials, the variant antibodies established in this study may be expected to be less immunogenic because it has been shown that some therapeutic fusion proteins that consist of combinations of natural sequences, such as tumor necrosis factor receptor/Fc (40) or LFA3/Fc (41), do not induce any profound antidrug responses in the clinic.

As a result of IgG1/IgG3 domain shuffling, three variants (1133, 3133, and 1333) showed enhanced CDC activity that was even more

**Table 1.** Summary of CDC activity mediated by anti-CD20 antibody variants

| Anti-CD20 antibody | Target: ST486 | | Target: Raji | |
|---|---|---|---|---|
| | $EC_{50}$ (μg/mL) | Maximal lysis (%) | $EC_{50}$ (μg/mL) | Maximal lysis (%) |
| IgG1wt(+f) | 0.246 ± 0.275 | 106.2 ± 11.1 | 35.7 ± 40.9 | 71.0 ± 14.1 |
| IgG1wt(−f) | 0.297 ± 0.315 | 95.5 ± 14.5 | 54.7 ± 61.2 | 44.1 ± 17.2 |
| IgG3wt(+f) | 0.178 ± 0.170 | 98.2 ± 5.25 | 1.89 ± 0.313 | 68.3 ± 21.7 |
| IgG3wt(−f) | 0.162 ± 0.158 | 102 ± 4.38 | 3.75 ± 2.44 | 71.5 ± 14.6 |
| 1133(+f) | 0.041 ± 0.020 | 107 ± 2.55 | 0.853 ± 0.158 | 100 ± 4.06 |
| 1133(−f) | 0.036 ± 0.023 | 108 ± 0.79 | 0.837 ± 0.238 | 99.1 ± 3.79 |
| 113F(+f) | 0.027 ± 0.008 | 113 ± 2.61 | 0.750 ± 0.235 | 99.2 ± 4.03 |
| 113F(−f) | 0.026 ± 0.010 | 103 ± 2.14 | 0.819 ± 0.216 | 96.3 ± 4.94 |
| IgG4wt(+f) | ND | 47.4 ± 1.26 | ND | 9.44 ± 12.9 |

NOTE: Mean values ± SD obtained from three independent experiments are shown. $EC_{50}$ and maximal lysis values are calculated by four-variable regression equations of each plot. Variant IgG4wt(+f), an IgG4-type rituximab (16), was used as a negative control.
Abbreviation: ND, not determined.

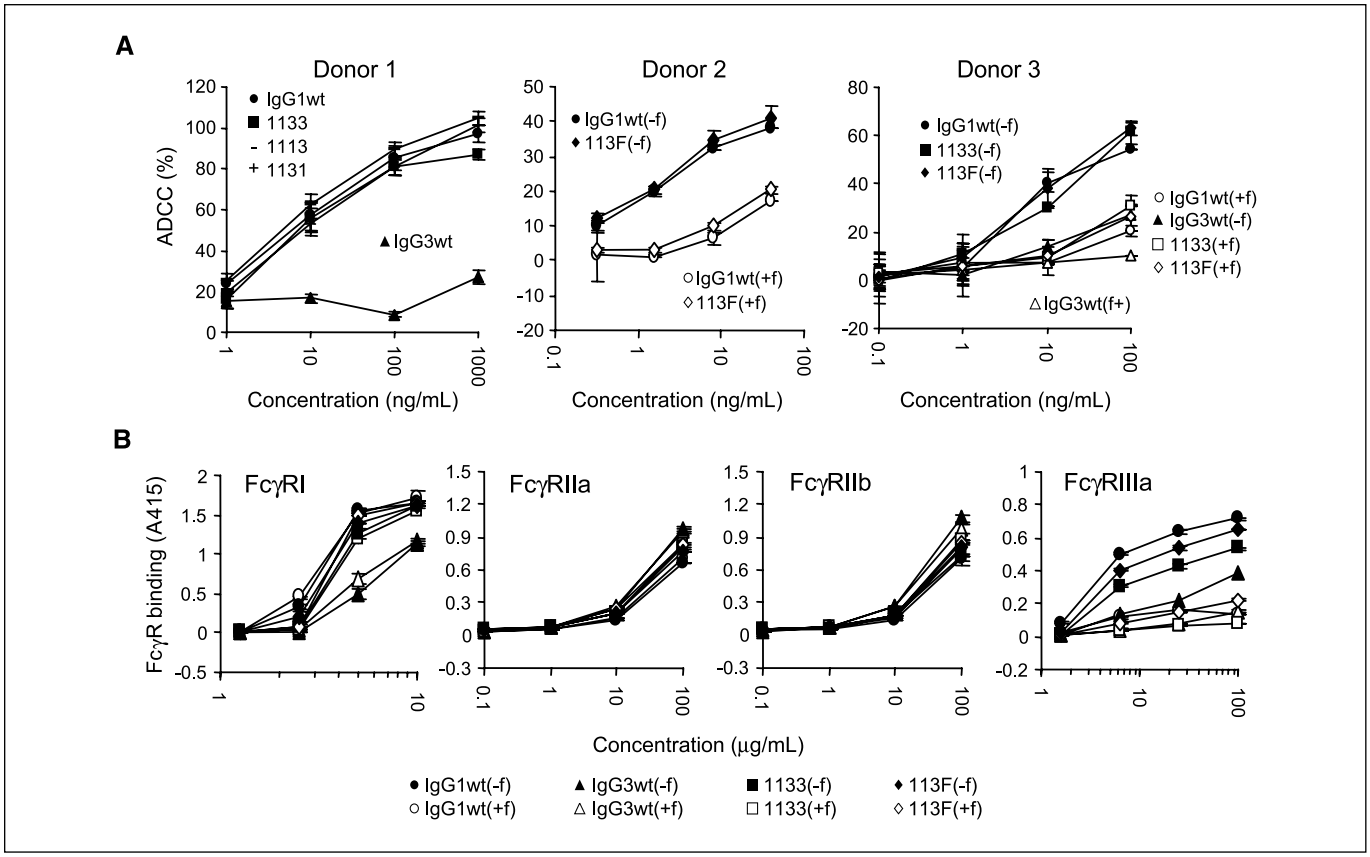


**Figure 4.** FcγR-mediated activity of the variant antibodies. All antibody samples shown have nonfucosylated glycoform if not otherwise specified, except in comparative studies of fucosylated and nonfucosylated antibodies [in such case, samples were denoted as (+f) and (−f) in the figures, respectively]. *A,* ADCC activity mediated by effector cells derived from three different blood donors. Raji cells were used as target cells. *Points,* mean of triplicates; *bars,* SD. *B,* binding profiles of anti-CD20 variant antibodies to FcγRI, FcγRIIa ($^{131}$His allotype), FcγRIIb, and FcγRIIIa ($^{158}$Val allotype). *Points,* mean of triplicates; *bars,* SD.

potent than the parent wild-type antibodies. The common structure among these variants is the Fc derived from IgG3. This should contribute to the potent CDC activity in part because IgG3 Fc has higher C1q-binding affinity than IgG1 Fc ($K_a = 2.9 \times 10^4$ and $1.2 \times 10^4$, respectively; ref. 24). Although the known C1q contact residues (Asp$^{270}$, Lys$^{322}$, Kys$^{326}$, Pro$^{329}$, Pro$^{331}$, and Glu$^{333}$; ref. 42), which constitute a cluster on the accessible surface of the CH2 domain, are conserved among IgG subclasses, amino acid residues adjacent to this region include polymorphic residues different between IgG1 and IgG3, such as Lys$^{274}$Gln, Asn$^{276}$Lys, and Tyr$^{300}$Phe, as shown by available structure of human IgG1 (PDB accession no. 1FC1). Therefore, it is likely that these residues have some roles in the relatively strong C1q binding of IgG3 isotype. However, the presence of the CH2 domain of IgG3, by itself, cannot explain entirely the augmented activity in the CDC-enhancing variants because they were even more potent than parent IgG3wt. The structural requirement for the enhanced CDC activity of the variants should be interpreted in the context of whole IgG structure. It seems likely that specific combinations of multiple IgG domains of different subclasses render the overall variant antibody structure capable of binding C1q with unexpectedly strong affinity.

Of the three initial variants with strong CDC (variants 3133, 1133, and 1333), the effect seen for the variant 3133 might be a consequence of shortening of the hinge region in IgG3, a phenomenon that increases C1q binding and CDC activity of IgG3 as revealed by Michaelsen et al. (22) and Brekke et al. (23). However, the degree of CDC enhancement seen in variant 3133 was modest in the anti-CD20 system used in this study. Although there is little information on the involvement of CH1 domain in CDC activity, interestingly, our results suggested that the CH1 domain derived from IgG1 was also a contributor to the maximal CDC activity because variant 1133, the best CDC inducer, exceeded 3133 in CDC activity. Further supporting this, another CDC-enhancing variant, 1333, also augmented the CDC activity of IgG3wt. Of note, Gaboriaud et al. (43) proposed a structural model in which the C1q head fits into a cleft formed between the CH2 and the Fab, suggesting that the Fab arm, in addition to the CH2, interacts with C1q (although this model favors rather the CL domain in the Fab as the contact site). As for the hinge, the influence of this domain on CDC activity was difficult to interpret from the results in this study, as there was no obvious tendency of enhanced CDC between variants with IgG1 hinge and IgG3 hinge region.

In further studies, we proceeded to modify the variant 1133 to provide protein A–binding capacity by reducing IgG3-derived portion without substantial reduction in its optimal CDC activity. The initial step was to determine which domain in the Fc was important for the CDC enhancement, revealing both the CH2 and the CH3 domains (both derived from IgG3) were involved, although the contribution of the CH2 domain is more significant, as revealed by comparing variants 1131 and 1113. Hence, we speculated further that the enhanced but suboptimal CDC activity of variant 1131,

which retained protein A–binding capacity, could further be improved by fine tuning of the CH3 domain (variants 113A to 113G). This was shown with variants 113E and 113F, with which both variants simultaneously exhibited protein A binding and near maximal CDC activity. It is unclear how each IgG3 residue in the CH3 domain affects complement activation despite their distal location from known C1q-binding sites. Among eight IgG3-specific residues in this domain (see Materials and Methods), two residues at positions 392 and 397 are located in the CH3:CH3 interface (44), whereas others are exposed on the surface of the molecule (shown by PDB 1FC1). Among variants 113A to 113G, there is a large increase in CDC especially between variants 113D and 113E (Fig. 3*B*), and interestingly, the only structural difference between them is Val$^{397}$Met alteration in 113E. It is possible that this change in hydrophobicity has some influence on the overall structure of IgG because interaction between the CH3 domains is important for the association of the two heavy chains (44, 45) and thus possibly affects C1q-binding property. On the other hand, other amino acid changes in the CH3 seem to have less effect on CDC than Val$^{397}$Met.

About the protein A binding, our results indicate that the presence of the CH3 of IgG1 isotype or, more specifically, His$^{435}$ (the only difference between variants 113F and 113G) is sufficient to retain this activity. This is consistent with the fact that replacing His$^{435}$ with Arg (the residue seen in IgG3) abrogates protein A binding of IgG (46), whereas other known contact sites with protein A (Thr$^{250}$, Ile$^{253}$, His$^{310}$, and Met$^{430}$) are common between IgG1 and IgG3 (47). Interestingly, this region (located in the CH2-CH3 cleft) spatially overlaps with the binding site to neonatal Fc receptor (FcRn), which is involved in IgG clearance, and variant 113F also possesses all known residues involved in FcRn binding, including His$^{435}$ (reviewed in ref. 48).

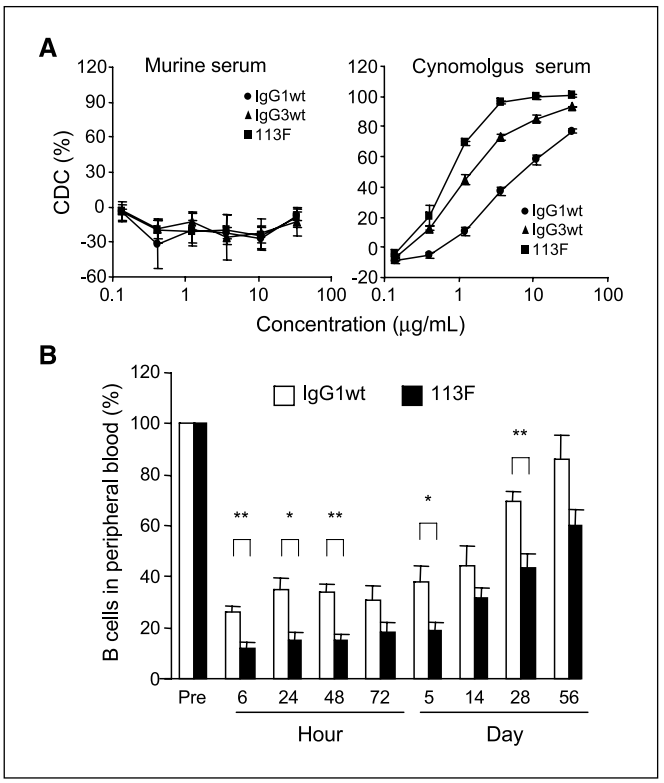


**Figure 5.** Animal study. All antibody samples shown have nonfucosylated glycoform. *A,* CDC activity using sera from nude mice (*left*) and a cynomolgus monkey (*right*) as complement source. For murine CDC, murine CD20/EL4-A cells were used as target to avoid the nonspecific killing of human cells by murine serum. For monkey CDC, Raji cells were used as target cells. *Points,* mean of triplicates; *bars,* SD. *B,* percent B cells remaining in peripheral blood of cynomolgus monkeys after single i.v. injection of IgG1wt (□) or variant 113F (■; $n = 4$ each, 0.1 mg/kg). *Columns,* mean; *bars,* SE. Significant differences between groups are indicated by * ($P < 0.05$) or ** ($P < 0.01$) as determined by two-tailed unpaired *t* test.

The CDC-enhancing effect by IgG1/IgG3 chimeric isotype was confirmed in multiple antigen systems (CD20 and CD52), both of which have been shown as successful therapeutic targets by rituximab and alemtuzumab. This suggests that the CDC-enhancing methodology described herein is not limited to a certain type of antigen but can be applied to wide range of target molecules.

Another important feature of the CDC-enhancing variants was that they were produced in CHO/*FUT8*$^{-/-}$ cells. The absence of fucose in their carbohydrate structure has been shown to promote maximal ADCC activity (49). The ADCC activity of these variants reached levels as potent as that achieved by nonfucosylated IgG1, which is considered to have fully saturated cytotoxicity compared with other mutational approaches that improves Fc:FcγRIIIa interaction (49).

The concept of the CDC-enhancing variants was further confirmed in a cynomolgus monkey, B-cell depletion model. Although anti-CD20 antibodies may have multiple cytotoxic mechanism *in vivo* (ADCC, CDC, phagocytosis, and apoptosis; reviewed in ref. 50), the result described herein suggests the enhanced *in vivo* cytotoxicity exerted by the variant 113F. In concordance with the previous observation of the rapid complement consumption from the sera of rituximab-treated patients (4), the current result might also suggest rapid kinetics of *in vivo* complement-mediated activity because the enhanced killing of blood B cells was observed at the first sample collection (6 h after injection). Importantly, the enhanced killing led to a significant delay in recovery, suggesting that the use of the variant constant region sequences may add to the therapeutic effect of conventional IgG1-type antibody therapeutics.

In conclusion, we have shown that systematic shuffling of IgG1/IgG3 isotypes can generate a set of variant antibodies with a variety of altered effector functions. Among these, the most attractive variants for therapy might be a set of heavy chain constant regions in which the Fc of IgG1 was partially converted to IgG3, possessing strong CDC-inducing capacity with full retention of ADCC activity and protein A–binding capacity. ADCC activities of these variants were further enhanced to the maximal levels when modified with nonfucosylated Fc-linked oligosaccharides. Antibodies possessing all of these attributes are of potentially great therapeutic value. Additional study will be necessary to examine the undetermined question whether the use of the variant constant regions alters pharmacokinetics and immunogenicity. Monkey studies on variant antibodies that are directed to antigens not abundantly expressed in normal tissues (unlike CD20) will enable the accurate assessment of the pharmacokinetic profile, although we observed that variant 113F showed very similar pharmacokinetic profile to that of IgG1 in mice and rats, whose endogenous CD20 molecules do not react with anti-human CD20 antibodies.[5] Future clinical trials will also confirm the hypothesis that the variant constant regions consist of fully natural amino acid sequences and oligosaccharides would render the antibodies

[5] Unpublished data.

potentially less immunogenic compared with artificial mutation approaches.

## Disclosure of Potential Conflicts of Interest

No potential conflicts of interest were disclosed.

## Acknowledgments

Received 11/19/2007; revised 2/11/2008; accepted 2/22/2008.

The costs of publication of this article were defrayed in part by the payment of page charges. This article must therefore be hereby marked *advertisement* in accordance with 18 U.S.C. Section 1734 solely to indicate this fact.

We thank Drs. George Spitalny and William Ofosu-Appiah for helpful suggestions and critical reading of the manuscript.

## References

1. Clynes RA, Towers TL, Presta LG, Ravetch JV. Inhibitory Fc receptors modulate *in vivo* cytoxicity against tumor targets. Nat Med 2000;6:443–6.
2. Cartron G, Dacheux L, Salles G, et al. Therapeutic activity of humanized anti-CD20 monoclonal antibody and polymorphism in IgG Fc receptor FcγRIIIa gene. Blood 2002;99:754–8.
3. Di Gaetano N, Cittera E, Nota R, et al. Complement activation determines the therapeutic activity of rituximab *in vivo*. J Immunol 2003;171:1581–7.
4. Kennedy AD, Beum PV, Solga MD, et al. Rituximab infusion promotes rapid complement depletion and acute CD20 loss in chronic lymphocytic leukemia. J Immunol 2004;172:3280–8.
5. Anolik JH, Campbell D, Felgar RE, et al. The relationship of FcγRIIIa genotype to degree of B cell depletion by rituximab in the treatment of systemic lupus erythematosus. Arthritis Rheum 2003;48:455–9.
6. Weng WK, Levy R. Two immunoglobulin G fragment C receptor polymorphisms independently predict response to rituximab in patients with follicular lymphoma. J Clin Oncol 2003;21:3940–7.
7. Kim DH, Jung HD, Kim JG, et al. FCGR3A gene polymorphisms may correlate with response to frontline R-CHOP therapy for diffuse large B-cell lymphoma. Blood 2006;108:2720–5.
8. Shields RL, Namenuk AK, Hong K, et al. High resolution mapping of the binding site on human IgG1 for FcγRI, FcγRII, FcγRIII, and FcRn and design of IgG1 variants with improved binding to the FcγR. J Biol Chem 2001;276:6591–604.
9. Lazar GA, Dang W, Karki S, et al. Engineered antibody Fc variants with enhanced effector function. Proc Natl Acad Sci U S A 2006;103:4005–10.
10. Umana P, Jean-Mairet J, Moudry R, Amstutz H, Bailey JE. Engineered glycoforms of an antineuroblastoma IgG1 with optimized antibody-dependent cellular cytotoxic activity. Nat Biotechnol 1999;17:176–80.
11. Shields RL, Lai J, Keck R, et al. Lack of fucose on human IgG1 N-linked oligosaccharide improves binding to human FcγRIII and antibody-dependent cellular toxicity. J Biol Chem 2002;277:26733–40.
12. Shinkawa T, Nakamura K, Yamane N, et al. The absence of fucose but not the presence of galactose or bisecting *N*-acetylglucosamine of human IgG1 complex-type oligosaccharides shows the critical role of enhancing antibody-dependent cellular cytotoxicity. J Biol Chem 2003;278:3466–73.
13. Miyoshi E, Uozumi N, Noda K, Hayashi N, Hori M, Taniguchi N. Expression of α1-6 fucosyltransferase in rat tissues and human cancer cell lines. Int J Cancer 1997;72:1117–21.
14. Niwa R, Hatanaka S, Shoji-Hosaka E, et al. Enhancement of the antibody-dependent cellular cytotoxicity of low-fucose IgG1 Is independent of FcγRIIIa functional polymorphism. Clin Cancer Res 2004;10:6248–55.
15. Niwa R, Shoji-Hosaka E, Sakurada M, et al. Defucosylated chimeric anti-CC chemokine receptor 4 IgG1 with enhanced antibody-dependent cellular cytotoxicity shows potent therapeutic activity to T-cell leukemia and lymphoma. Cancer Res 2004;64:2127–33.
16. Niwa R, Natsume A, Uehara A, et al. IgG subclass-independent improvement of antibody-dependent cellular cytotoxicity by fucose removal from $Asn^{297}$-linked oligosaccharides. J Immunol Methods 2005;306:151–60.
17. Natsume A, Wakitani M, Yamane-Ohnuki N, et al. Fucose removal from complex-type oligosaccharide enhances the antibody-dependent cellular cytotoxicity of single-gene-encoded antibody comprising a single-chain antibody linked the antibody constant region. J Immunol Methods 2005;306:93–103.
18. Shoji-Hosaka E, Kobayashi Y, Wakitani M, et al. Enhanced Fc-dependent cellular cytotoxicity of Fc fusion proteins derived from TNF receptor II and LFA-3 by fucose removal from Asn-linked oligosaccharides. J Biochem 2006;140:777–83.
19. Yamane-Ohnuki N, Kinoshita S, Inoue-Urakubo M, et al. Establishment of FUT8 knockout Chinese hamster ovary cells: an ideal host cell line for producing completely defucosylated antibodies with enhanced antibody-dependent cellular cytotoxicity. Biotechnol Bioeng 2004;87:614–22.
20. Idusogie EE, Wong PY, Presta LG, et al. Engineered antibodies with increased activity to recruit complement. J Immunol 2001;166:2571–5.
21. Dall'Acqua WF, Cook KE, Damschroder MM, Woods RM, Wu H. Modulation of the effector functions of a human IgG1 through engineering of its hinge region. J Immunol 2006;177:1129–38.
22. Michaelsen TE, Aase A, Westby C, Sandlie I. Enhancement of complement activation and cytolysis of human IgG3 by deletion of hinge exons. Scand J Immunol 1990;32:517–28.
23. Brekke OH, Bremnes B, Sandin R, Aase A, Michaelsen TE, Sandlie I. Human IgG3 can adopt the disulfide bond pattern characteristic for IgG1 without resembling it in complement mediated cell lysis. Mol Immunol 1993;30:1419–25.
24. Schumaker VN, Calcott MA, Spiegelberg HL, Muller-Eberhard HJ. Ultracentrifuge studies of the binding of IgG of different subclasses to the Clq subunit of the first component of complement. Biochemistry 1976;15:5175–81.
25. Bruggemann M, Williams GT, Bindon CI, et al. Comparison of the effector functions of human immunoglobulins using a matched set of chimeric antibodies. J Exp Med 1987;166:1351–61.
26. Lutz R, Michael C, Herman W, Greg W. Reshaping human antibodies for therapy. Nature 1988;332:323–7.
27. Zuckier LS, Chang CJ, Scharff MD, Morrison SL. Chimeric human-mouse IgG antibodies with shuffled constant region exons demonstrate that multiple domains contribute to *in vivo* half-life. Cancer Res 1998;58:3905–8.
28. Tao MH, Canfield SM, Morrison SL. The differential ability of human IgG1 and IgG4 to activate complement is determined by the COOH-terminal sequence of the CH2 domain. J Exp Med 1991;173:1025–8.
29. Canfield SM, Morrison SL. The binding affinity of human IgG for its high affinity Fc receptor is determined by multiple amino acids in the CH2 domain and is modulated by the hinge region. J Exp Med 1991;173:1483–91.
30. Tan LK, Shopes RJ, Oi VT, Morrison SL. Influence of the hinge region on complement activation, C1q binding, and segmental flexibility in chimeric human immunoglobulins. Proc Natl Acad Sci U S A 1990;87:162–6.
31. Norderhaug L, Brekke OH, Bremnes B, et al. Chimeric mouse human IgG3 antibodies with an IgG4-like hinge region induce complement-mediated lysis more efficiently than IgG3 with normal hinge. Eur J Immunol 1991;21:2379–84.
32. Urlaub G, Mitchell PJ, Kas E, et al. Effect of γ rays at the dihydrofolate reductase locus: deletions and inversions. Somat Cell Mol Genet 1986;12:555–66.
33. Niwa R, Sakurada M, Kobayashi Y, et al. Enhanced natural killer cell binding and activation by low-fucose IgG1 antibody results in potent antibody-dependent cellular cytotoxicity induction at lower antigen density. Clin Cancer Res 2005;11:2327–36.
34. Kabat EA, Wu TT, Perry H, Gottesman K, Foeller C. Sequences of proteins of immunological interest. 5th ed. NIH Publication No. 91-3242. Bethesda (MD): NIH; 1991.
35. Reff ME, Carner K, Chambers KS, et al. Depletion of B cells *in vivo* by a chimeric mouse human monoclonal antibody to CD20. Blood 1994;83:435–45.
36. Crowe JS, Hall VS, Smith MA, Cooper HJ, Tite JP. Humanized monoclonal antibody CAMPATH-1H: myeloma cell expression of genomic constructs, nucleotide sequence of cDNA constructs and comparison of effector mechanisms of myeloma and Chinese hamster ovary cell-derived material. Clin Exp Immunol 1992;87:105–10.
37. Golay J, Manganini M, Rambaldi A, Introna M. Effect of alemtuzumab on neoplastic B cells. Haematologica 2004;89:1476–83.
38. Bergman I, Basse PH, Barmada MA, Griffin JA, Cheung NK. Comparison of *in vitro* antibody-targeted cytotoxicity using mouse, rat and human effectors. Cancer Immunol Immunother 2000;49:259–66.
39. Jefferis R, Lund J, Mizutani H, et al. A comparative study of the N-linked oligosaccharide structures of human IgG subclass proteins. Biochem J 1990;268:529–37.
40. Cobo-Ibanez T, Martin-Mola E. Etanercept: long-term clinical experience in rheumatoid arthritis and other arthritis. Expert Opin Pharmacother 2007;8:1373–97.
41. Liu CM, McKenna JK, Krueger GG. Alefacept: a novel biologic in the treatment of psoriasis. Drugs Today 2004;40:961–74.
42. Idusogie EE, Presta LG, Gazzano-Santoro H, et al. Mapping of the C1q binding site on rituxan, a chimeric antibody with a human IgG1 Fc. J Immunol 2000;164:4178–84.
43. Gaboriaud C, Juanhuix J, Gruez A, et al. The crystal structure of the globular head of complement protein C1q provides a basis for its versatile recognition properties. J Biol Chem 2003;278:46974–82.
44. Ridgway JB, Presta LG, Carter P. 'Knobs-into-holes' engineering of antibody CH3 domains for heavy chain heterodimerization. Protein Eng 1996;9:617–21.
45. Deisenhofer J. Crystallographic refinement and atomic models of a human Fc fragment and its complex with fragment B of protein A from *Staphylococcus aureus* at 2.9- and 2.8-Å resolution. Biochemistry 1981;20:2361–70.
46. Medesan C, Matesoi D, Radu C, Ghetie V, Ward ES. Delineation of the amino acid residues involved in transcytosis and catabolism of mouse IgG1. J Immunol 1997;158:2211–7.
47. Kim JK, Firan M, Radu CG, et al. Mapping the site on human IgG for binding of the MHC class I-related receptor, FcRn. Eur J Immunol 1999;29:2819–25.
48. Roopenian1 DC, Akilesh S. FcRn: the neonatal Fc receptor comes of age. Nat Rev Immunol 2007;7:715–25.
49. Masuda K, Kubota T, Kaneko E, et al. Enhanced binding affinity for FcγRIIIa of fucose-negative antibody is sufficient to induce maximal antibody-dependent cellular cytotoxicity. Mol Immunol 2007;44:3122–31.
50. Smith MR. Rituximab (monoclonal anti-CD20 antibody): mechanisms of action and resistance. Oncogene 2003;22:7359–68.

# Engineered Antibodies of IgG1/IgG3 Mixed Isotype with Enhanced Cytotoxic Activities

Akito Natsume, Mika In, Hiroyuki Takamura, et al.

*Cancer Res* 2008;68:3863-3872.